

Article

Low-Carbon Transition Pathway Planning of Regional Power Systems with Electricity-Hydrogen Synergy

Liang Ran, Yaling Mao ^{*}, Tiejiang Yuan and Guofeng Li 

School of Electrical Engineering, Dalian University of Technology, Dalian 116024, China

^{*} Correspondence: maoyaling@mail.dlut.edu.cn

Abstract: Hydrogen energy leads us in an important direction in the development of clean energy, and the comprehensive utilization of hydrogen energy is crucial for the low-carbon transformation of the power sector. In this paper, the demand for hydrogen energy in various fields is predicted based on the support vector regression algorithm, which can be converted into an equivalent electrical load when it is all produced from water electrolysis. Then, the investment costs of power generators and hydrogen energy equipment are forecast considering uncertainty. Furthermore, a planning model is established with the forecast data, initial installed capacity and targets for carbon emission reduction as inputs, and the installed capacity as well as share of various power supply and annual carbon emissions as outputs. Taking Gansu Province of China as an example, the changes of power supply structure and carbon emissions under different scenarios are analysed. It can be found that hydrogen production through water electrolysis powered by renewable energy can reduce carbon emissions but will increase the demand for renewable energy generators. Appropriate planning of hydrogen storage can reduce the overall investment cost and promote a low carbon transition of the power system.

Keywords: hydrogen energy; low-carbon transition; long-term planning; electricity-hydrogen synergy



Citation: Ran, L.; Mao, Y.; Yuan, T.; Li, G. Low-Carbon Transition Pathway Planning of Regional Power Systems with Electricity-Hydrogen Synergy. *Energies* **2022**, *15*, 8764. <https://doi.org/10.3390/en15228764>

Academic Editor: Muhammad Aziz

Received: 8 October 2022

Accepted: 18 November 2022

Published: 21 November 2022

Publisher's Note: MDPI stays neutral with regard to jurisdictional claims in published maps and institutional affiliations.



Copyright: © 2022 by the authors. Licensee MDPI, Basel, Switzerland. This article is an open access article distributed under the terms and conditions of the Creative Commons Attribution (CC BY) license (<https://creativecommons.org/licenses/by/4.0/>).

1. Introduction

The Paris Agreement has set a long-term goal for global climate change governance, limiting global temperature rise to well below 2 °C, and preferably to 1.5 °C [1]. A low-carbon transition in the power sector is key to tackling climate change. Reduction of carbon emissions further in the power sector relies mainly on the integrated application of multiple low-carbon technologies [2,3], including wind, solar, nuclear, biomass and other renewable energy generation technologies; carbon capture, storage and utilisation technologies; and biomass coupled carbon capture technologies [4,5]. Among them, hydrogen energy technology is one of the most important low-carbon technologies [6], which has attracted much attention in China in recent years, especially since the introduction of carbon peaking and carbon neutral targets, and relevant policies are also promoting the development of hydrogen energy technology. In terms of application scenarios, the utilisation of hydrogen is mainly concentrated in four principal areas: industry, electricity, transport and building heating, as well as functioning as industrial raw materials, means of energy storage and alternative fuels. The hydrogen demand will continue to rise in all areas in the future [7]. The research for hydrogen energy includes the physical component and the integrated energy system. The physical component involves the electrolyzer, the hydrogen fuel cell, and the storage and transport carrier [8]. Several papers have reviewed the current developments in them. This paper focuses on integrated energy systems from a planning perspective [9,10].

Ref. [11] proposes a regional electricity-hydrogen integrated energy system that uses the coupling of electricity and hydrogen to improve renewable energy utilisation and a double layer mixed integer planning model aimed at reducing the levelized cost of hydrogen by optimising the proportion of wind and photovoltaic power generation installed

in the system and the electricity purchased via the grid. Ref. [12] note that integrated expansion planning of power, natural gas, and hydrogen systems will contribute to the decarbonization of energy systems and identify the combination of technologies that meet energy demands and carbon emission reduction targets with optimal economics. Ref. [13] presents a novel methodology for optimising investment costs by linking two energy system models, the application of which demonstrates that hydrogen can greatly assist in the transition to complete decarbonization of the heating process, as it is able to provide clean heat for a relatively low investment. All the above articles illustrate that transitioning to hydrogen energy will lead technology in an important direction in the development of clean energy; the installations related to hydrogen should be planned combined with regional renewable sources, which can contribute effectively to the economics of the system and facilitate the transition to low carbon heating.

In the context of the transition to low carbon heating, research on simulation methods for energy and power system evolution and multi-temporal load forecasting methods has intensified [14,15]. In the early stage, related literature mainly used integrated assessment models to study the decarbonisation paths of the energy and power sectors, with a focus on fine-grained simulation for a particular year or rough planning for the long term, lacking joint optimisation combining long-term planning and short-term fine-grained dispatch [16]. Most of the literature now establishes joint optimisation models for long-term planning and short-term operation, considering production simulations to achieve power balance constraints on electricity [17]. The literature [18] established a long-term planning method for power systems with high spatial and temporal resolution and technical accuracy based on four base scenarios, namely the policy scenario, the enhanced scenario, the 2 °C scenario, and the 1.5 °C scenario proposed by the Climate Institute of Tsinghua University [19], considering the time-level power balance and the spatial matching problems, and forming a joint planning-operation optimisation model. The literature [20] further established a full-chain techno-economic evaluation model of diversified new energy utilisation methods for comparative analysis of long-term development paths, following the analysis of near- and medium-term planning. However, few existing studies have adequately considered the integrated application of hydrogen energy for long term planning, despite its immense potential for application in the low carbon transition of regional energy systems, mainly due to the lack of historical data on hydrogen energy and the immaturity of the market [21].

Therefore, in this paper, by analysing the comprehensive hydrogen energy utilisation model, the SVR model is used to forecast the future hydrogen energy demand and electrical load in the medium- and long-term based on various social data published by official agencies and to convert the hydrogen load into its equivalent electrical load. Combined with the current situation in the planning area, the Ito model is used to forecast the cost of power generation technology and the cost of key equipment for hydrogen energy systems. Then, based on the above predictions, a low-carbon transition planning model of the regional power system is established. After simulation and analysis, a feasible path to achieve low carbon transition using hydrogen energy is proposed.

2. Prediction of Hydrogen Load and Uncertainty Parameter

Currently, hydrogen is mainly produced from fossil fuels such as coal, oil, and natural gas, in addition to water electrolysis and biomass gasification. Ninety-six% of the world's hydrogen is produced from fossil fuels [22]. The carbon emission of different hydrogen production methods varies, depending on which hydrogen produced can be classified as grey hydrogen, blue hydrogen, and green hydrogen [23], as shown in Figure 1 [24].

With the rapid development of renewable energy generation technologies, green hydrogen replaces grey and blue hydrogen as an important way to save energy and reduce emissions. As shown in Figure 2, hydrogen is produced in diverse ways, then stored and transported for use in hydrogen fuel cells for power generation, gas turbines for energy generation, industrial ammonia and alcohol production, steel and oil refining, etc. The different utilisation modes are adapted to different scenarios, with the main hydrogen

utilisation modes in the thermal, transport and industrial sectors being (a,b–e) and (a–c,d–f) in the power sector in Figure 2.

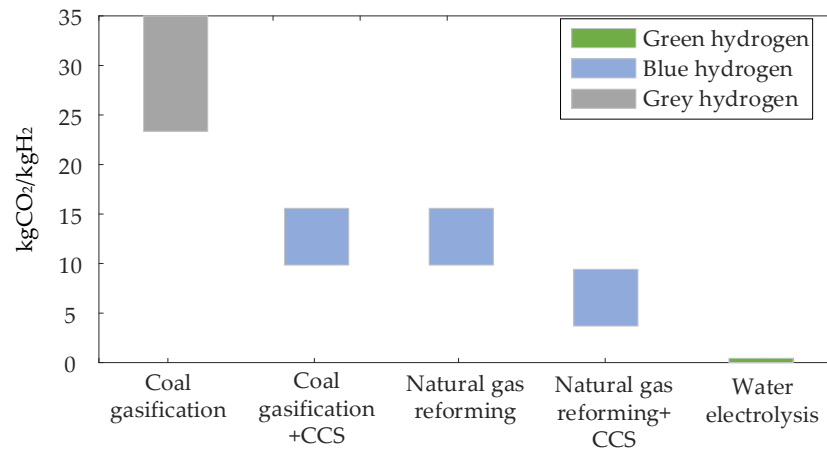


Figure 1. Comparison of the carbon emissions of different hydrogen production methods.

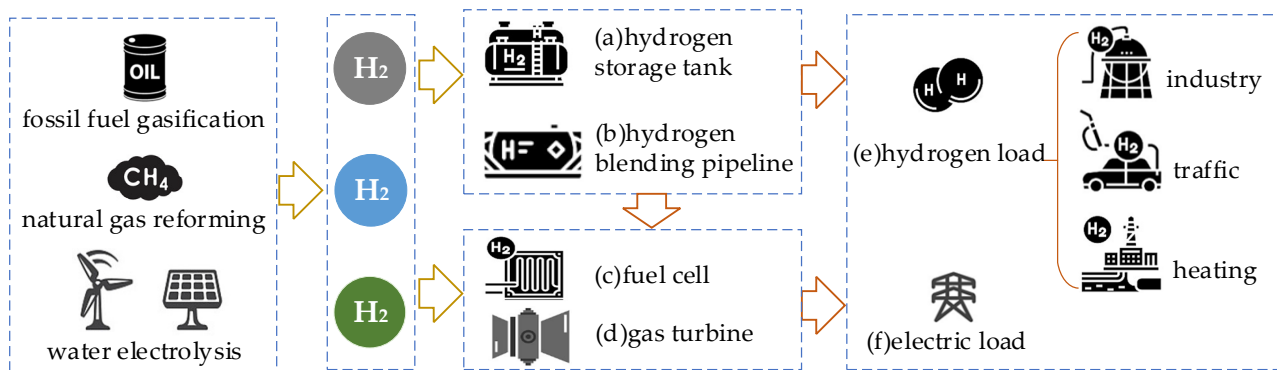


Figure 2. Comprehensive utilization of hydrogen energy.

2.1. Prediction of Hydrogen Load

In the process of low carbon transformation of the power system, green hydrogen has a wide range of applications in the industrial, construction and transportation sectors. The demand for hydrogen in industry is mainly for regional ammonia and methanol synthesis and crude oil processing; the demand for hydrogen in transport is mainly for city buses when they are all hydrogen fuel cell vehicles; and the demand for hydrogen in buildings is mainly for blending with hydrogen for heating in city natural gas pipelines [23].

The demand for hydrogen energy on a medium- to long-term time scale can be projected from the above three sectors, and the relevant data can be obtained from the China Statistical Yearbook 2021 published on the website of the National Bureau of Statistics [25]. In the industrial sector, the amount of hydrogen required in a calendar year is calculated based on the annual processing of crude oil and the annual production of ammonia, methanol, and empirical constants; in the transportation sector, the hydrogen load for transportation is calculated using historical data on bus ownership, assuming that future buses will use hydrogen as a power fuel; in the building sector, based on data on the supply of natural gas to cities, the hydrogen load is calculated in a calendar year, assuming that hydrogen is blended at a rate of 5% by volume fraction. The hydrogen load for building heating is shown in Equation (1).

$$HD_{y,ind} = \eta_{oil}Q_{y,oil} + \eta_{amm}Q_{y,amm} + \eta_{alc}Q_{y,alc} \tag{1}$$

$$HD_{y,trans} = \eta_{fuel}d_{aver}Q_{y,bus} \tag{2}$$

$$HD_{y,heat} = \eta_{gas}Q_{y,ng} \quad (3)$$

where $HD_{y,ind}$, $HD_{y,trans}$, $HD_{y,heat}$ are the hydrogen loads in the industrial, transport, and municipal heating sectors in year y . $Q_{y,oil}$, $Q_{y,bus}$, $Q_{y,ng}$ denote the crude oil processing, ammonia and methanol generation in year y . η_{oil} , η_{amm} , η_{alc} denote the hydrogen consumption coefficient for crude oil processing, ammonia synthesis and methanol, with reference to literature [26] for the values. d_{aver} and η_{fuels} are the average annual mileage and fuel consumption factor of buses respectively [27]. η_{gas} is the proportion of natural gas blended with hydrogen [28].

Based on the historical data obtained, the hydrogen load for each year was predicted using the support vector regression (SVR) method [29] for the different areas.

2.2. Equivalent Electric Load of Hydrogen

Green hydrogen is obtained by electrolysis of water from renewable energy sources, so the hydrogen equivalent replacement electrical load can be obtained by converting Equations (2) and (3).

$$P_{eq,t} = (e_{eq} + e_{com})HD_t \quad (4)$$

$$HD_t = HD_{t,ind} + HD_{t,trans} + HD_{t,heat} \quad (5)$$

where $P_{eq,t}$ is the equivalent electric load of hydrogen at time t ; kW·h and HD_t denote the hydrogen load at time t ; kg, e_{eq} and e_{com} are the energy consumption for electrolysis and compression of hydrogen; kW·h/kg. $HD_{t,ind}$, $HD_{t,trans}$, $HD_{t,heat}$ are the hydrogen loads in the industrial, transport, and municipal heating sectors at time t .

2.3. Investment Cost Forecasts for Key Equipment

The Ito process is an important fundamental theory for analysing the evolutionary properties of stochastic dynamic systems. It uses stochastic differential equations to describe randomness, which can better describe the probability distribution and time series correlation of randomness [30], and is commonly used in the financial field to describe the long-term trend of stock prices, oil prices, exchange rates, etc. Its application in power systems has also been increasing in recent years. The Ito process describes the random variables as the following stochastic differential equations.

$$dX_t = \mu(X_t)dt + \sigma(X_t)dB_t \quad (6)$$

where, X_t and t are the random variables, $d(\cdot)$ denotes its differential. $\mu(X_t)$ is drift rate, $\sigma(X_t)$ is fluctuation rate, and B_t denotes Brownian motion (or Wiener process).

Ito process simulation with linear drift rate and volatility is used to forecast the costs of power generation technologies and hydrogen energy equipment in this paper, where price fluctuations can be assumed to be:

$$dX_t = \mu X_t dt + \sigma X_t dB_t \quad (7)$$

where, μ and σ are the means and variances of price fluctuations.

In the time interval, according to the Ito Lemma, there is:

$$d \ln X_t = (\mu - \sigma^2/2)dt + \sigma dB_t \quad (8)$$

where, $\ln X_t$ is the logarithm of X_t .

Since the expression for Brownian motion is Equation (7), Equation (6) in discrete form it can be expressed as Equation (8).

The mean and standard deviations of the logarithm of the forecast volume is estimated from historical data, and this price movement can then be modelled using the above formula. The price curve predicted by this method considers uncertainty, which can arise from policy changes, market fluctuations, and technology maturity.

3. Transition Path Planning Model with Electro-Hydrogen Synergy

The input data to the model includes the installed capacity in the initial year (2020), the forecasted electricity and hydrogen loads, and the fuel prices and carbon trading prices over the planning cycle, which are calculated and outputted by the medium- and long-term planning model. The process is shown in Figure 3.

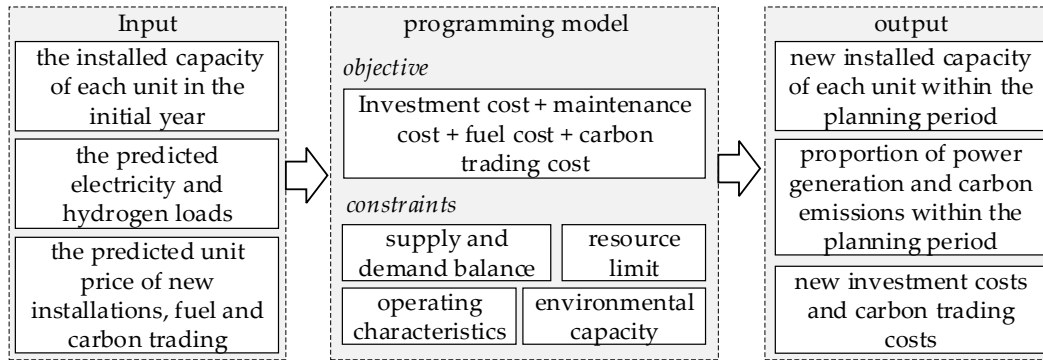


Figure 3. The planning process.

3.1. Objective

The objective function is the lowest total cost of the power system during the planning period, including the investment cost of the power supply, the hydrogen energy system, the system operation and maintenance cost, the fuel cost F_{fc} , and the carbon trading cost F_{ct} , as shown in Equations (9)–(13).

$$F = \sum_{y=1}^T (F_{inv.y} + F_{om.y} + F_{fc.y} + F_{ct.y}) (1 + I)^{-y} \quad (9)$$

$$F_{inv.y} = (\sum_g cap_{y,g} Nb_{y,g} + \sum_s cap_{y,s} Nb_{y,s}) \quad (10)$$

$$F_{om.y} = k(\sum_g cap_{y,g} IC_{y,g} + \sum_s cap_{y,s} IC_{y,s}) \quad (11)$$

$$F_{fc.y} = \sum_t f_c p_{y,f} P_{y,t,C} \quad (12)$$

$$F_{ct.y} = p_{y,c} (cem_y - cea_y) \quad (13)$$

where F is the objective function of the planning model, $T = 30$ is the planning cycle. I is the discount rate. The subscript y indicates the y th year from 2020, i.e., 2020 $y = 1$. The subscript g indicates the type of power and $g \in \{C, H, W, PV\}$ which denotes thermal power, hydroelectricity, wind power, photovoltaic power, respectively. The subscript s indicates the equipment of hydrogen energy and $s \in \{EC, HS, FC\}$, which denotes electrolytic cell, hydrogen storage tank and fuel cell, respectively. $F_{inv.y}$, $F_{om.y}$, $F_{fc.y}$, $F_{ct.y}$ are investment costs, operation and maintenance costs, fuel costs, and carbon trading costs in year y , respectively. $cap_{y,g/s}$ is the price per unit of installed capacity in year y . $Nb_{y,g/s}$ is the additional installed capacity in year y . $IC_{y,g/s}$ is the installed capacity in year y . $P_{y,t,C}$ is the power of thermal power units at time t in year y . $p_{y,f}$ is the price of fuel in year y . f_c is fuel consumption factor per unit. cem_y and cea_y are the carbon emissions and initial carbon allowances in year y , respectively. $p_{y,c}$ is the price of carbon trading in year y .

3.2. Constraints

Supply and demand balance satisfies the constraints of Equations (14) and (15)

$$\sum_g P_{y,t,g} + P_{y,t,EC1} - P_{y,t,FC} = D_{y,t} \quad (14)$$

$$P_{eq,t,y} = P_{y,t,EC2} \quad (15)$$

where $P_{y,t,g/EC1/EC2/FC}$ denotes the power of unit $g/EC1/EC2/FC$ at time t in year y . $D_{y,t}$ is the electricity load at time t in year y . $EC1$ is electrolysis cell for hydrogen energy storage, and $EC2$ is used to meet the hydrogen load.

The power is limited as in Equations (16)–(18)

$$per_{y,g,min} IC_{y,g} \leq P_{y,t,g} \leq per_{y,g,max} IC_{y,g} \quad (16)$$

$$p_{down} \leq P_{y,t,C} - P_{y,t-1,C} \leq p_{up} \quad (17)$$

$$per_{EC,min} IC_{y,EC} \leq P_{y,t,EC1} + P_{y,t,EC2} \leq per_{EC,max} IC_{y,EC} \quad (18)$$

where $per_{y,g,max/min}$ is the maximum/minimum output coefficients of renewable energy. $p_{up/down}$ is the up and down climbing factors for thermal power units. $per_{EC,max/min}$ is maximum/minimum output coefficients of the hydrogen energy storage.

The energy storage state constraints are Equations (19)–(23)

$$0 \leq SOC_{y,t,HS} \leq IC_{y,HS} \quad (19)$$

$$SOC_{y,t+1,HS} = SOC_{y,t,HS} + \eta_s V_{y,t,HSc} + V_{y,t,HSd}/\eta_s \quad (20)$$

$$V_{y,t,HSc} = \eta_{EC} P_{y,t,EC1} \quad (21)$$

$$V_{y,t,HSd} = \eta_{FC} P_{y,t,FC} \quad (22)$$

$$SOC_{y,t,HS,0} = SOC_{y,t,HS,T} = \delta_s IC_{y,HS} \quad (23)$$

where $SOC_{y,t,HS}$ are the state of charge of hydrogen energy storage. $\eta_{EC/FC}$ is gas-electric conversion factor of electrolysis and fuel cell. η_s denotes the loss factor of energy storage. $SOC_{y,t,HS,0}$ and $SOC_{y,t,HS,T}$ are the initial and final state, respectively. δ_s is the maximum state factor of energy storage.

The constraints of carbon emission are Equation (24).

$$0 \leq cem_y \leq CEM_y \quad (24)$$

where, CEM_y is the maximum carbon emissions in year y to meet the carbon neutrality target in 2050.

4. Case Study

In this section, a regional power system in Gansu Province, China, is used for simulation and analysis as an example. The hydrogen load and electrical load are predicted in Section 4.1 according to the method of Sections 2.1 and 2.2, and unit investment costs for hydrogen energy equipment and power generation equipment are forecasted in Section 4.2 based on the model of Section 2.3. Then, based on the above predicted data and the model in Section 3, simulations were carried out under three assumed scenarios and the results are presented in Section 4.3, where the planning results for power and hydrogen plants are shown in Sections 4.3.1 and 4.3.2, the annual carbon emissions calculated from the planning results are shown in Section 4.3.3, and the operation results for four typical days in 2030 and 2050 are shown in Section 4.3.4.

4.1. Results of the Load Forecast

Hydrogen demand forecasting is conducted using hydrogen load data for industry, transport and municipal heating, and social data in Gansu Province, China. The social data are shown in Table 1, and the hydrogen load data for each sector for the calendar year, considering the per capita GNP, the share of primary industry, the share of secondary industry, the share of tertiary industry, the gross regional product, the total population, the number of urban population, the number of rural population, the total retail sales of consumer goods and the total social electricity consumption, are shown in Table 2.

Table 1. Social data.

Year	Gross Regional Output Value per Capita	Share of Primary Industry	Share of Secondary Industry	Share of Tertiary Industry	Gross Regional Product	Total Population	Urban Population	Rural Population	Total Retail Sales of Social Consumer Goods	Total Social Electricity Consumption
2007	10,346	14.3	47.3	38.4	2702.4	2548	822	1726	833.3	614.74
2008	12,110	14.6	46.3	39.1	3166.8	2551	856	1695	1023.6	677.76
2009	12,872	14.7	45.1	40.2	3387.6	2555	891	1664	1183.0	705.51
2010	16,113	14.5	48.2	37.3	4120.7	2560	925	1635	1394.5	804.43
2011	19,595	13.5	47.4	39.1	5020.4	2564	953	1612	1648.0	923.45
2012	21,978	13.8	46.0	40.2	5650.2	2578	999	1579	1906.5	994.56
2013	24,539	14.0	45.0	41.0	6330.7	2582	1036	1546	2368.8	1073.25
2014	26,433	13.2	42.8	44.0	6836.8	2591	1080	1511	2668.3	1095.48
2015	26,165	14.1	36.7	49.2	6790.3	2599	1123	1477	2907.2	1098.72
2016	27,643	13.7	34.9	51.4	7200.4	2610	1166	1444	3184.4	1065.15
2017	28,496	11.5	34.3	54.1	7459.9	2626	1218	1408	3426.6	1164.37
2018	31,336	11.2	33.9	54.9	8104.1	2637	1258	1379	3428.3	1289.52
2019	32,994	12.0	32.8	55.1	8718.3	2647	1284	1363	3700.3	1288
2020	35,995	13.3	31.6	55.1	9016.7	2502	1307	1195	3632.4	1376

Table 2. Historical data on hydrogen loads in various fields.

Year	Methanol (Tonnes)	Ammonia (Tonnes)	Crude Oil Processing Volume (10^4 tun)	Buses	Total City Gas Supply (Billion Cubic Metres)
2007	57,687	777,460.5	/	/	/
2008	62,062	658,704.5	/	/	/
2009	54,008.3	761,022.8	/	/	/
2010	50,514.72	763,833.1	1383.5	4382	7.29
2011	364,619.9	733,376	1613.5	4965	8.81
2012	564,232	431,337.9	1520.5	5214	11.21
2013	506,165.3	700,655.1	1554.2	5359	13.4
2014	727,115.9	575,393	1446.4	5488	15.92
2015	/	/	1424.3	5275	16.19
2016	/	/	1341.5	5233	16.86
2017	/	/	1440.8	5850	20.37
2018	/	/	1440	6519	23.51
2019	/	/	1465.6	7314	25.2
2020	/	/	1467.5	6408	25.44

The hydrogen loads in the industrial, transport and building heating sectors from 2020 to 2050 are predicted by the SVR model as shown in Figure 4.

To reflect the demand balance between electricity and hydrogen, the seasonal and hourly variability of renewable energy sources, and to minimise the difficulty of calculation, one typical day from each of the four seasons of the year was selected for simulation. The hydrogen loads in the transport and municipal heating sectors are more regular, and the industrial hydrogen volumes fluctuate less throughout the year, so the normalised results of the hourly variation of hydrogen loads in each sector are shown in Figure 5.

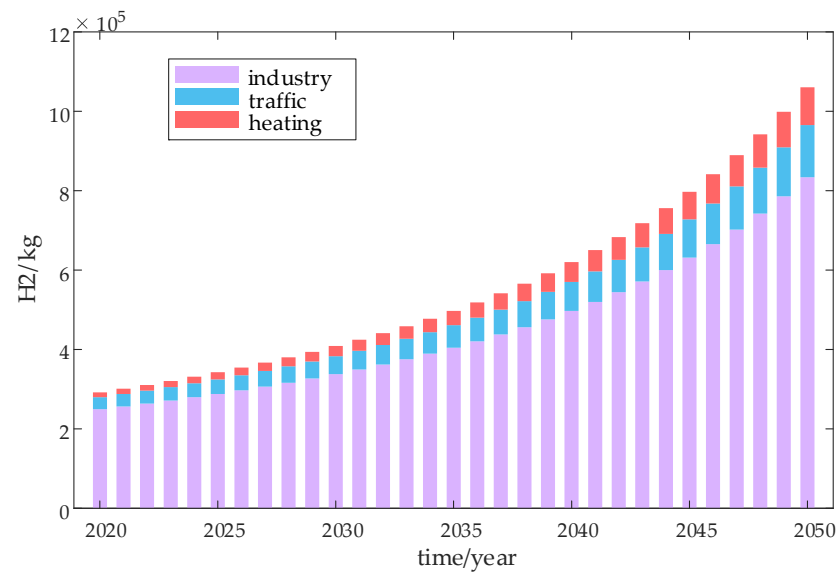


Figure 4. Prediction curve of annual hydrogen load.

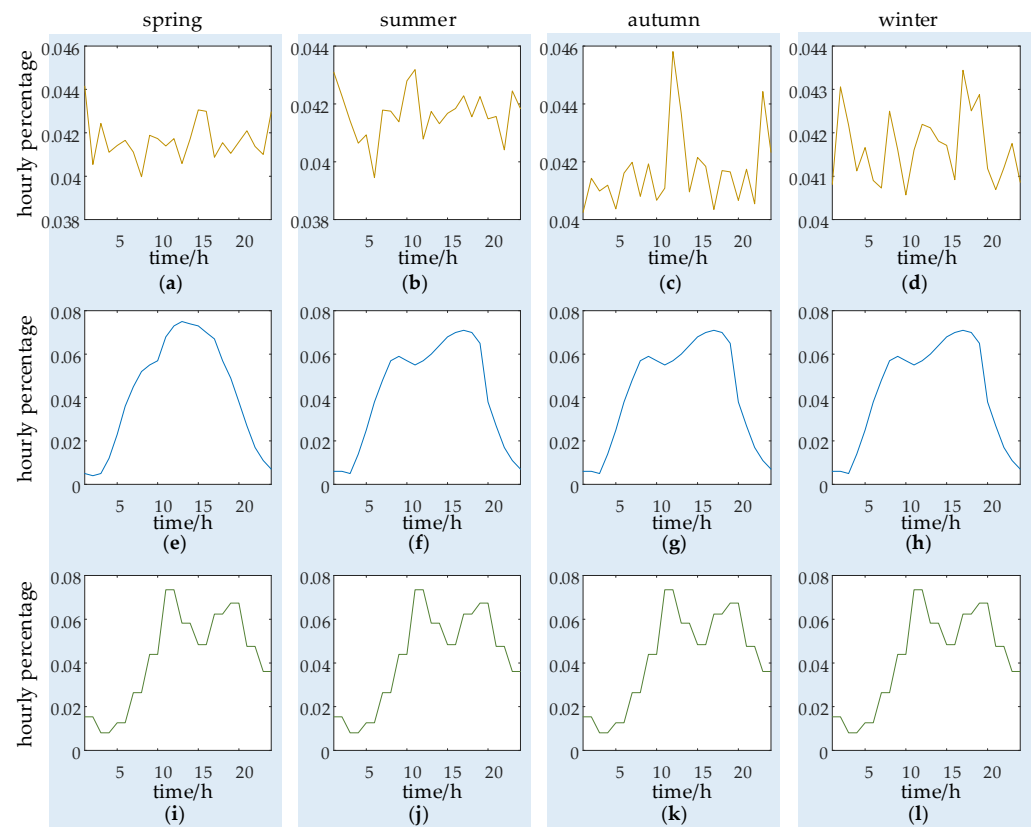


Figure 5. Hourly percentage of hydrogen load in different area for four seasons. (a–d) industrial hydrogen load; (e–h) traffic hydrogen load; (i–l) hydrogen load for heating.

The annual electrical load forecast for the region is shown in Figure 6. Based on the maximum load for each month from 2018 to 2021, a typical day can be selected from each of January, April, July, and November, and the load curve is shown in Figure 7.

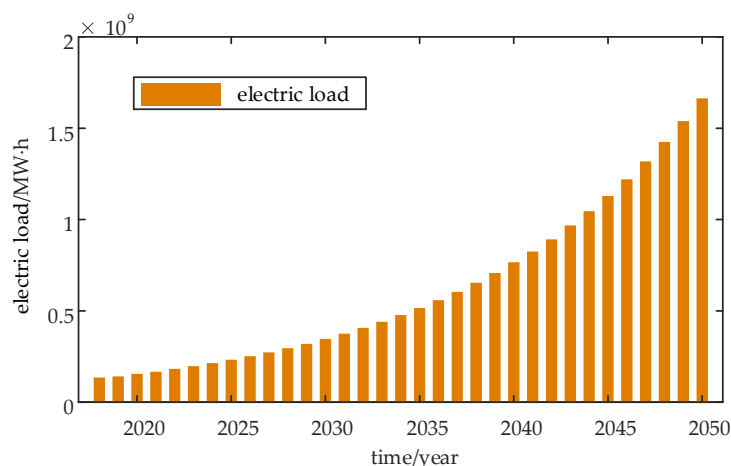


Figure 6. Forecasted annual electrical load from 2020 to 2050.

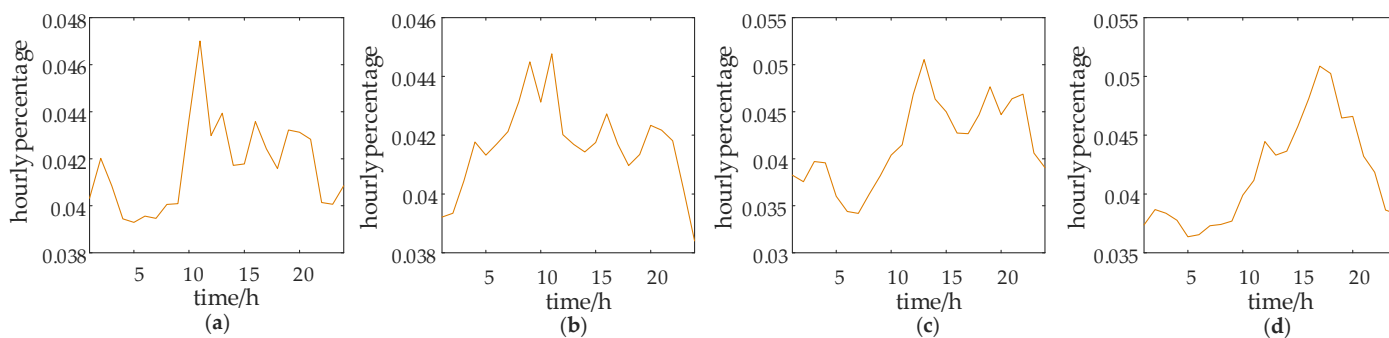


Figure 7. Hourly percentage of electric load in four seasons. (a) spring; (b) summer; (c) autumn; (d) winter.

4.2. Forecasted Equipment Investment Costs

By investigating the various types of data and related technological developments published by official agencies, the relevant data on key hydrogen energy equipment and power generation costs are summarised as shown in Tables 3 and 4, and the Ito process of linear drift rate and volatility is used for simulation to predict the future trend of changes in hydrogen energy system costs and unit power generation investment costs as shown in Figures 8 and 9.

Table 3. Hydrogen energy equipment investment costs over the years.

Equipment	2016	2018	2020	2022
Alkaline electrolytic cell	3000~4000	3000~4000	2000~3000	2000~3000
Hydrogen storage tank	5000~6000	4000~5000	3000~4000	3000~4000
Fuel cell	6000~7000	5000~6000	4000~5000	4000~5000

Table 4. Power generation equipment investment costs over the years.

Power	2016	2018	2020	2022
Wind power	2000~3000	down 24~30%	down 37~49%	2000~3000
Photovoltaic power	1000~3000	down 24~30%	down 50~60%	1000~3000
Hydroelectricity	7000~8000	down 0.2~1%	down 0.2~1%	7000~8000
Thermal power	4000~8000	up 0~10%	up 10~30%	4000~8000

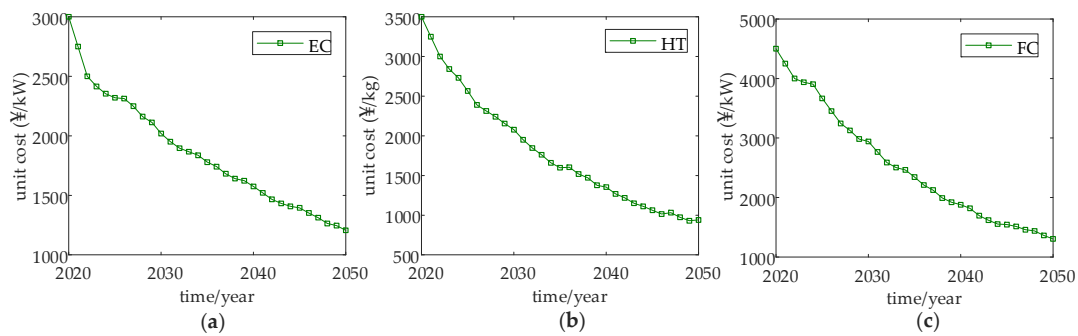


Figure 8. Forecasted price curves for hydrogen energy equipment from 2020 to 2050. (a) electrolytic cell; (b) hydrogen storage tank; (c) fuel cell.

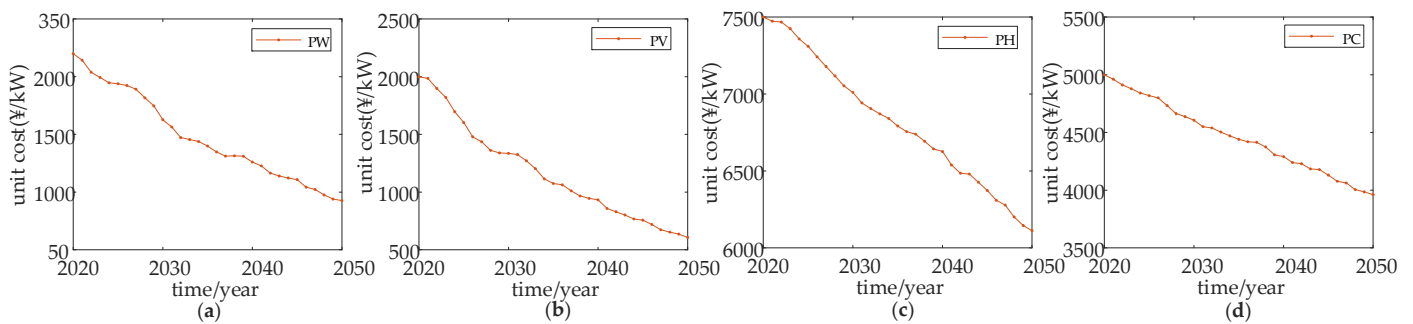


Figure 9. Forecasted investment costs for power generation technologies. (a) wind power; (b) solar power; (c) hydroelectricity; (d) thermal power.

4.3. Comparative Analysis of Planning Paths

The following three scenarios are set up for a comparative analysis:

- Scenario 1: no hydrogen load is considered
- Scenario 2: considering hydrogen-equivalent electrical loads in industry, transport and heating
- Scenario 3: considering hydrogen load and hydrogen storage in power systems

The installed capacity of wind, photovoltaic, hydropower and thermal power in the region in 2021 is 17,331.2, 10,743.5, 9,316.3, and 20,389.7 MW, respectively. The model built in Section 3 is run through the YALMIP toolbox of the MATLAB platform and the GUROBI solver is invoked, where the three scenarios took 32.05 s, 40.20 s, and 65.51 s, respectively.

4.3.1. Growth in Installed Capacity of Generations

The planning results, such as the installed capacity of and share of the power sources, are obtained by inputting the forecast data from Sections 4.1 and 4.2 into the model in Section 3 and solving it. The changes in the installed capacity and share of the four main power sources under the three scenarios are shown in Figure 10. When the comprehensive use of hydrogen energy is not considered, the planning results are shown in Figure 10a,b. In the long term, the proportion of new energy installations will continue to rise, and the share of wind and photovoltaic in the power supply is 82% in 2030 and 91% in 2050. There will be no need for new coal installations after 2025. The power supply structure will shift to mainly new energy generation, supplemented by thermal power units, and thermal power units will be gradually retired, eventually reducing the installed capacity to zero in 2050. This is also due to the gradual reduction in the cost of wind power and photovoltaic power generation technologies. As the cost of wind power is higher than that of photovoltaic in the early years, there is more room for technological upgrading in the later years, so the installed capacity of wind power will exceed that of photovoltaic after 2032, with a greater rise. The installed capacity of hydropower will increase more slowly due to geographical

constraints and the maturity of power generation technology. But it will rise significantly after 2040, mainly due to the retirement of thermal power and the growth of new energy generation, which requires a more stable power supply. The installed capacity of wind power, photovoltaic and hydropower is over 20 times, 34 times, and 8 times than in 2021, respectively, and more than 6 times, 5 times, and 4 times in 2030, respectively.

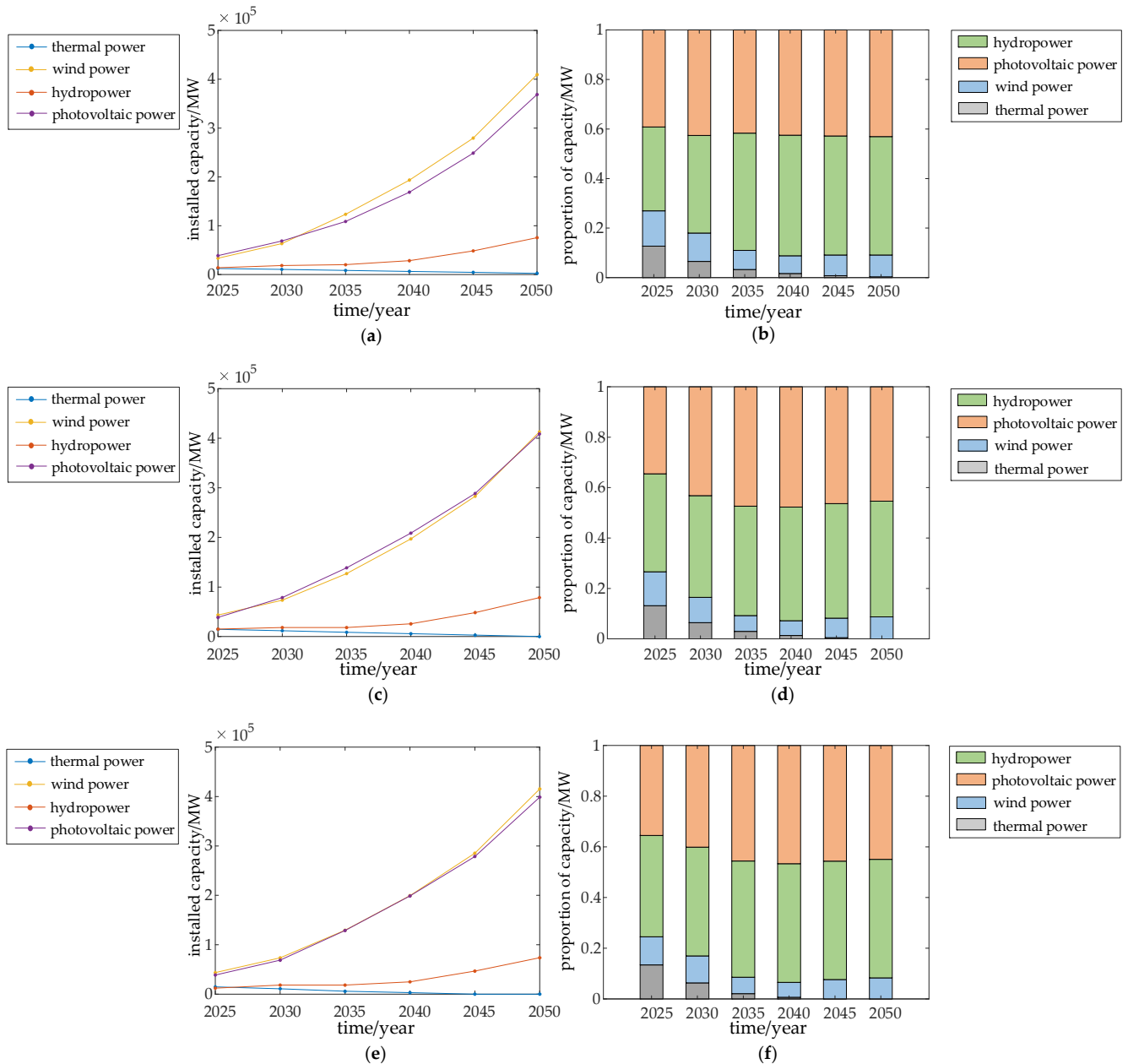


Figure 10. The installed capacity of and share of the power sources. (a,b) scenario 1; (c,d) scenario 2; (e,f) scenario 3.

In scenario 2, the integrated use of hydrogen energy is considered, and traditional grey hydrogen and blue hydrogen are replaced with hydrogen produced from electricity. Based on this, the planning results are shown in Figure 10c,d. Compared to scenario 1, the replacement of grey and blue hydrogen with green hydrogen will help to accelerate the pace of achieving the carbon neutrality target. The increased electrical load from hydrogen replacement is likely to increase the pressure on the power system to reduce emissions, but by relying on renewable energy to generate hydrogen and considering the

CO₂ reductions in the three sectors, the benefits of hydrogen replacement are much greater than the cost of increasing some of the electrical loads compared to the emissions reductions in the three sectors. The 5.7736×10^{10} tonnes of carbon emission are reduced by green hydrogen replacement in industry, transport and heating, which relieves the pressure to cut emissions across the region. Wind power and photovoltaic doubled 23 times and 38 times, respectively, from 2021 to 2050, and their share will reach 91.3% in 2050.

In scenario 3, with the consideration of hydrogen storage in the power system and the equivalent electrical load for hydrogen demand, there is a slight increase in the installed capacity of PV and wind power compared to scenario 2, especially for wind power between 2030 and 2045, while installed capacity of hydropower grows more in 2030–2035 than in Scenario 2. The addition of hydrogen storage allows more capacity to be put into wind power, which is more stochastic and volatile, and thermal power to cease to be used for a power supply in 2045. The share of wind and photovoltaic power is 46.7% and 65.28% in 2045, respectively, an increase of 16 times and 23 times, respectively, compared to 2021. This multiplier increases to 24 and 37 in 2050.

4.3.2. Equipment of Hydrogen Energy System

In scenarios 2 and 3, the hydrogen energy equipment is configured based on the hydrogen load demand, and the results of the capacity planning for the electrolyzers and hydrogen storage tank are shown in Figures 11 and 12, respectively. Electrolyzer power increases from 2140 MW in 2025 to 5020 MW in 2050 in scenario 2, and from 3210 to 7530 MW in scenario 3. Correspondingly, the capacity of hydrogen storage tanks rises from 34,668 MW·h in 2025 to 130,520 MW·h in 2050 in scenario 2, and from 46,520 MW·h to 321,880 MW·h in scenario 3. The combination of hydrogen production and storage equipment can make the power of the electrolyser smoother, effectively reducing equipment capacity requirements and investment costs.

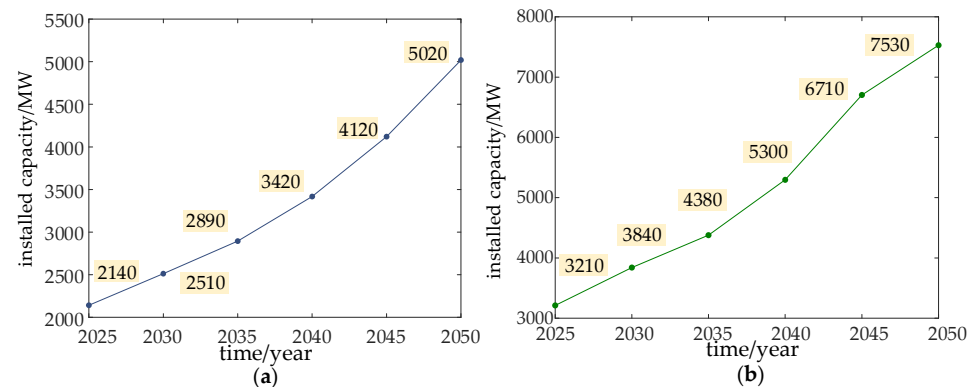


Figure 11. The planning capacity of electrolysis. (a) scenario 2; (b) scenario 3.

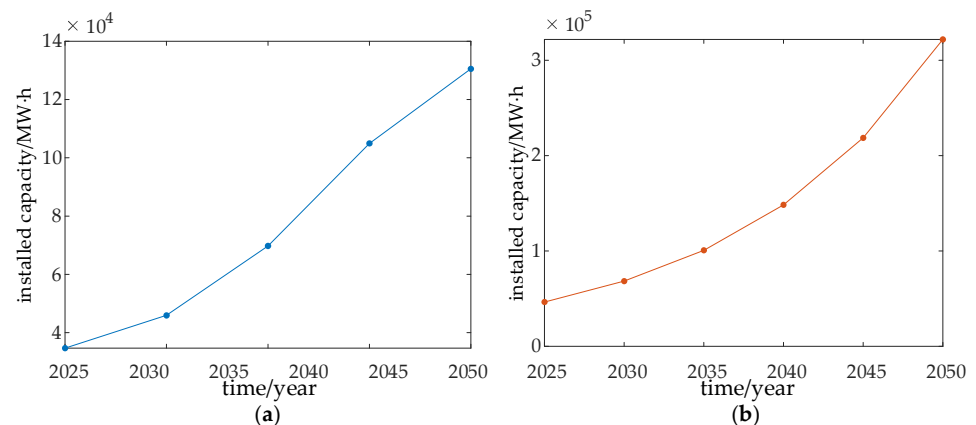


Figure 12. The planning capacity of hydrogen storage tank. (a) scenario 2; (b) scenario 3.

4.3.3. Cost and Carbon Emission

The addition of hydrogen equipment has increased investment costs and O&M costs; however, to achieve the goal of carbon neutrality, the substitution of grey hydrogen in industry, transport, and heating with electricity is necessary. In this context, it is clearly better that the path of hydrogen storage is considered in scenario 3, which has a lower total cost than scenario 2, as shown in Table 5. The carbon emission reduction from replacing grey hydrogen with green hydrogen is calculated by referring to the 1kg of hydrogen produced from coal to produce 20 kg of CO₂.

Table 5. The cost and carbon emission reduction of three scenarios.

Scenario	1	2	3
Investment cost/¥	1.4296×10^{12}	1.5083×10^{12}	1.4680×10^{12}
O&M cost/¥	8.1523×10^{10}	8.3701×10^{10}	8.2015×10^{10}
Total cost/¥	1.5111×10^{12}	1.5921×10^{12}	1.5499×10^{12}
Carbon emission/tun	15.1610×10^7	12.3655×10^7	11.7114×10^7
Emission reductions from hydrogen substitution/tun	/	5.7736×10^{10}	5.7736×10^{10}

Figure 13 shows the trend in carbon emissions, from which we can see that the period from 2025 to 2040 is the main period for reducing emissions. In scenario 2, the rate of emission reduction is slightly slower until 2035 than in scenario 1, but faster after 2035, when hydrogen loading is considered. Scenario 3 has consistently the fastest rate of emission reductions due to the role of hydrogen storage in the power system.

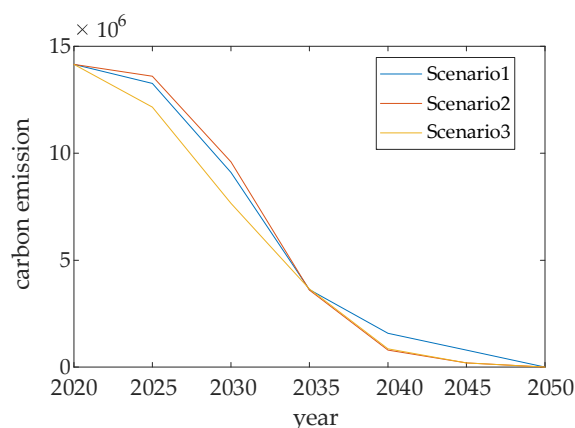


Figure 13. The results of carbon emission reduction.

4.3.4. Simulation Results of Daily Operation

This section focuses on the results of the operational simulation under scenario 3, analysing four typical days in 2030 and 2050 selected according to the output characteristics of wind power, and the results of the optimised operation are shown in Figures 14–16. The operation simulation is mainly to ensure that the planning results of the power supply and energy storage are sufficient to cope with the uncertainty of renewable energy during the daily operation. As can be seen in Figure 14, the output time of PV is more stable, usually between 9–18 h, and the energy storage is generally in a charged state during this period. The power output characteristics of wind power differ on the four typical days, with thermal power and storage mainly affected by it, while the hydropower output is smoother. As seen in Figure 15, in 2050 wind power will be the main source of power, followed by PV, with hydro and storage assisting them in supplying power.

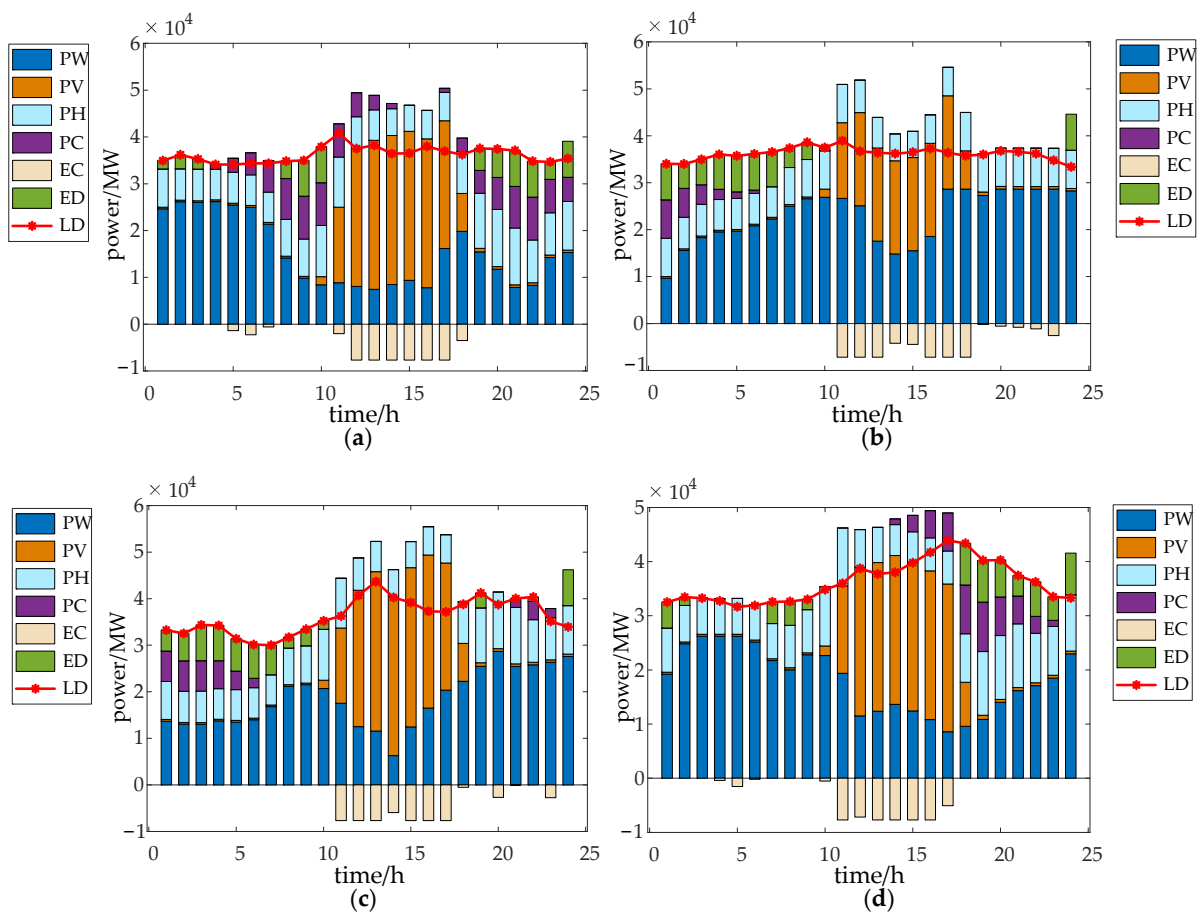


Figure 14. The operational results in 2030. (a) typical day 1; (b) typical day 2; (c) typical day 3; (d) typical day 4.

When renewable energy is more abundant during the 10–18 h period, the energy is stored and discharged through storage to maintain a balance between supply and demand when power is insufficient. This is the case for almost every typical day in 2030. However, in 2050, energy is also stored between 1–10 h on typical days 1 and 4, and between 16–23 h on typical days 2 and 3, due to the large share of renewables that require storage to work for longer periods.

The capacity state of the energy storage system is shown in Figure 16. As can be seen in the figure, the energy storage on typical days 2 and 3 in these two years is discharged in the 1–10 h period and is charging in the 10–24 h period almost. The difference in the operation state of the energy storage on typical days 1 and 4 in 2030 and 2050 is slightly larger, but in the 10–18 h period is also charging, and in the 7–10 h and 18–24 h periods is discharging. This is related to the output characteristics of wind power and photovoltaic, especially wind power, which has greater uncertainty, so there is a greater difference in the operating state of energy storage between 1 and 8 h.

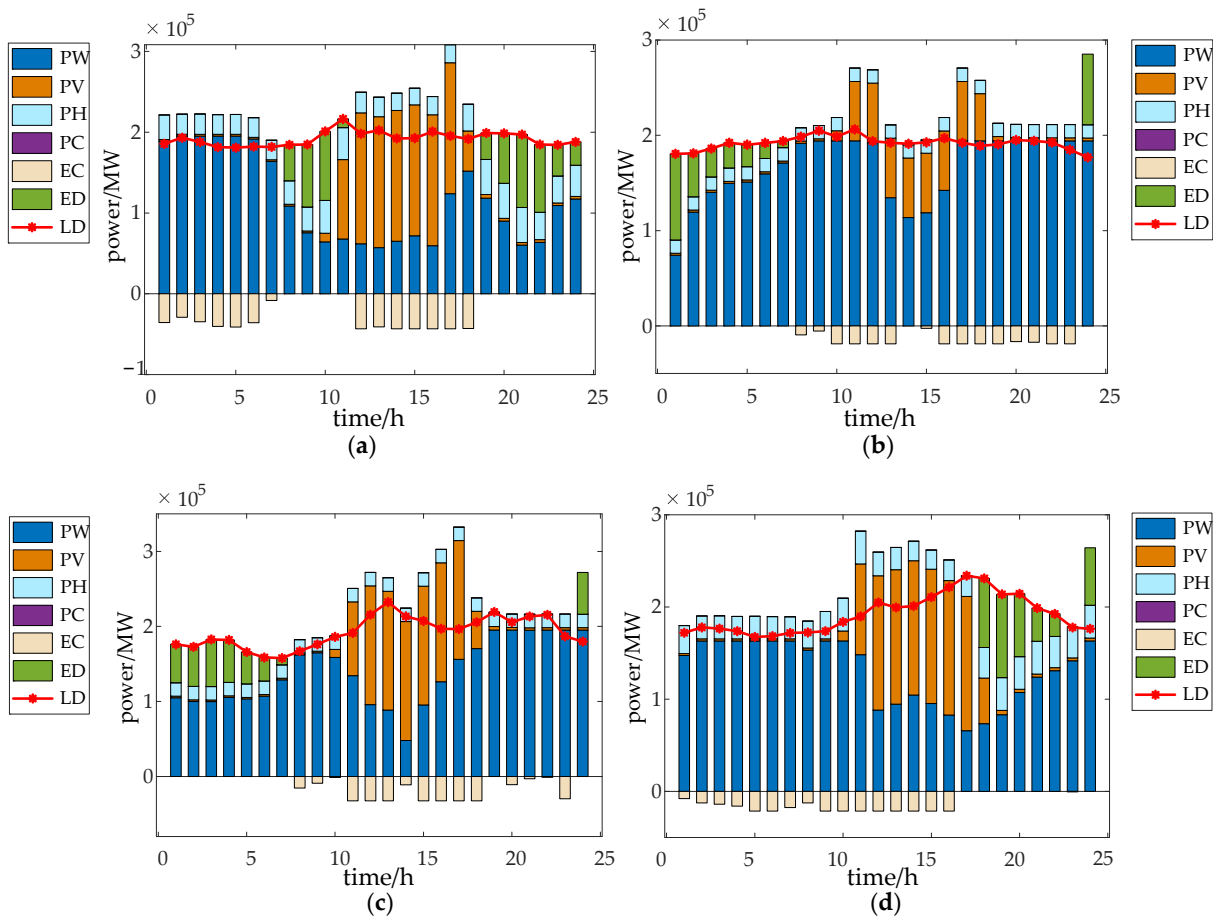


Figure 15. The operational results in 2050. (a) typical day 1; (b) typical day 2; (c) typical day 3; (d) typical day 4.

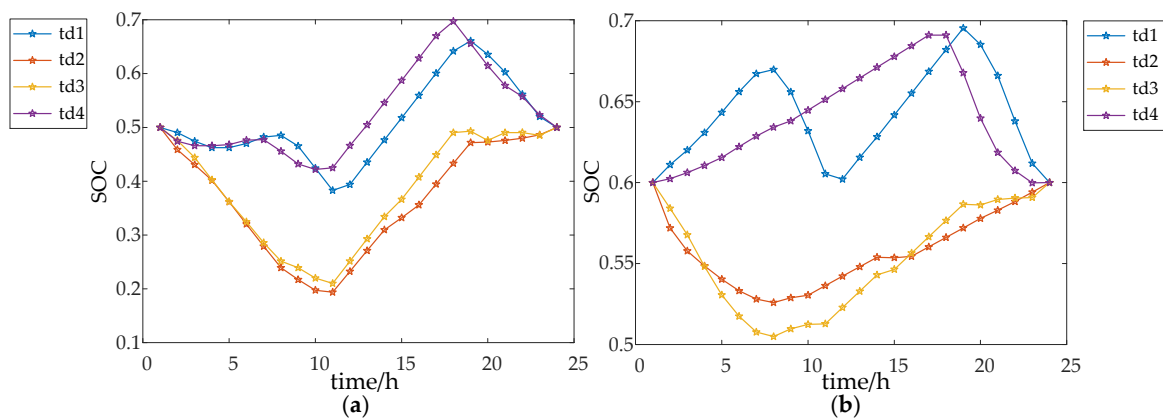


Figure 16. The state of charge on four typical days in 2030 and 2050. (a) 2030; (b) 2050.

5. Conclusions

Hydrogen energy is in great demand in industry, transportation, and heating. The replacement of grey hydrogen by green hydrogen will reduce a large amount of carbon dioxide in the hydrogen production process. In addition, the importance of hydrogen storage in the power system is gradually emerging as the proportion of renewable energy increases. In this paper, a long-term low-carbon transition path planning model is proposed for the regional power system considering short-term operation simulation, and the transition path is analysed according to three scenarios: (1) without hydrogen load; (2) considering

hydrogen load and converting it into equivalent electric load; (3) considering electric load derived from hydrogen load and hydrogen energy storage.

The load forecasts show a continued rise in hydrogen demand in the future. Planning for the future power structure with consideration of water electrolysis powered by renewable energy to hydrogen production could reduce a significant amount of carbon emissions. In our example, this value is 5.7736×10^{10} , which is hundreds of times the carbon emissions from electricity generation without considering hydrogen production from electricity. Therefore, the low carbon transition of the power system cannot only consider the traditional electric load, but also the electric load from hydrogen demand of other sectors, especially the industry sector. However, after considering electric hydrogen production, the rising electrical load makes the demand for renewable energy sources grow; the installed capacity of wind power and photovoltaics needs to increase to 23 and 38 times that of 2021, with both accounting for up to 91% of the total. This would entail huge investment costs.

Hydrogen energy storage, with its long-term, large-scale storage characteristics, will help the consumption of renewable energy and increase the equivalent utilization time. With its help, the increase in installed capacity of wind and photovoltaic is 16 and 23 times greater, and their share reaches 46% and 65% in 2050, respectively. In the two scenarios above, in 2050, the demand for electrolyzer capacity is 5020 MW and 27530 MW, respectively, and for hydrogen storage tank capacity is 130,520 MW·h and 321,880 MW·h, respectively. Operational simulations can ensure that the planning results are adequate, at least on typical days with different wind and photovoltaic power output characteristics; it is clear that energy storage is continuously charged or discharged for more than 6 h during the day. The role of energy storage in promoting the consumption of renewable energy cannot be ignored.

Furthermore, it can be observed that 2025 to 2035 is the main period for emission reduction. Seventy percent of the targeted emission reductions are achieved during this period. Greater investment in low-carbon technologies can accelerate the achievement of a low-carbon transition, such as electrolysis water to hydrogen technology, carbon capture, storage and utilisation technology, and large-scale energy storage technology, etc. This paper focuses on the role of hydrogen energy in the low-carbon transition, while the integration and use of more low-carbon technologies are yet to be discussed.

Author Contributions: Methodology, L.R.; Software, Y.M.; Supervision, G.L.; Project administration, T.Y. All authors have read and agreed to the published version of the manuscript.

Funding: This research received no external funding.

Conflicts of Interest: The authors declare no conflict of interest.

References

1. Klatzer, T.; Bachhiesl, U.; Wogrin, S. State-of-the-art expansion planning of integrated power, natural gas, and hydrogen systems. *Int. J. Hydrog. Energy* **2022**, *47*, 20585–20603. [[CrossRef](#)]
2. White, M.T.; Bianchi, G.; Chai, L.; Tassou, S.A.; Sayma, A.I. Review of supercritical CO₂ technologies and systems for power generation. *Appl. Therm. Eng.* **2021**, *185*, 116447. [[CrossRef](#)]
3. Zappa, W.; Junginger, M.; van den Broek, M. Is a 100% renewable European power system feasible by 2050? *Appl. Energy* **2019**, *233–234*, 1027–1050. [[CrossRef](#)]
4. Yang, E.; Mohamed, H.O.; Park, S.-G.; Obaid, M.; Al-Qaradawi, S.Y.; Castaño, P.; Chon, K.; Chae, K.-J. A review on self-sustainable microbial electrolysis cells for electro-biohydrogen production via coupling with carbon-neutral renewable energy technologies. *Bioresour. Technol.* **2021**, *320*, 124363. [[CrossRef](#)]
5. Wilberforce, T.; Olabi, A.; Sayed, E.T.; Elsaid, K.; Abdelkareem, M.A. Progress in carbon capture technologies. *Sci. Total Environ.* **2021**, *761*, 143203. [[CrossRef](#)] [[PubMed](#)]
6. Parra, D.; Valverde, L.; Pino, F.J.; Patel, M.K. A review on the role, cost and value of hydrogen energy systems for deep decarbonisation. *Renew. Sustain. Energy Rev.* **2019**, *101*, 279–294. [[CrossRef](#)]
7. Witkowski, A.; Rusin, A.; Majkut, M.; Stolecka, K. Analysis of compression and transport of the methane/hydrogen mixture in existing natural gas pipelines. *Int. J. Press. Vessel. Pip.* **2018**, *166*, 24–34. [[CrossRef](#)]

8. Thomas, J.M.; Edwards, P.P.; Dobson, P.J.; Owen, G.P. Decarbonising energy: The developing international activity in hydrogen technologies and fuel cells. *J. Energy Chem.* **2020**, *51*, 405–415. [[CrossRef](#)] [[PubMed](#)]
9. Rajalakshmi, N.; Balaji, R.; Ramakrishnan, S. Recent developments in hydrogen fuel cells: Strengths and weaknesses. In *Sustainable Fuel Technologies Handbook*, 14th ed.; Suman, D., Chaudhery, M.H., Eds.; Academic Press: New York, NY, USA, 2021; pp. 431–456. [[CrossRef](#)]
10. Lin, R.; Lu, Y.; Xu, J.; Huo, J.; Cai, X. Investigation on performance of proton exchange membrane electrolyzer with different flow field structures. *Appl. Energy* **2022**, *326*, 120011. [[CrossRef](#)]
11. Pan, G.; Gu, W.; Qiu, H.; Lu, Y.; Zhou, S.; Wu, Z. Bi-level mixed-integer planning for electricity-hydrogen integrated energy system considering leveled cost of hydrogen. *Appl. Energy* **2020**, *270*, 115176. [[CrossRef](#)]
12. Aunedi, M.; Yliruka, M.; Dehghan, S.; Pantaleo, A.M.; Shah, N.; Strbac, G. Multi-model assessment of heat decarbonisation options in the UK using electricity and hydrogen. *Renew. Energy* **2022**, *194*, 1261–1276. [[CrossRef](#)]
13. Net Zero by 2050, A Roadmap for the Global Energy Sector. Available online: https://iea.blob.core.windows.net/assets/deebef5d-0c34-4539-9d0c-10b13d840027/NetZeroBy2050-ARoadmapfortheGlobalEnergySector_CORR.pdf (accessed on 6 October 2022).
14. Zhang, Y.Z.; Zhang, X.P.; Lan, L.H. Robust optimization-based dynamic power generation mix evolution under the carbon-neutral target. *Resour. Conserv. Recycl.* **2022**, *178*, 106103. [[CrossRef](#)]
15. Jin, X.-B.; Zheng, W.-Z.; Kong, J.-L.; Wang, X.-Y.; Bai, Y.-T.; Su, T.-L.; Lin, S. Deep-Learning Forecasting Method for Electric Power Load via Attention-Based Encoder-Decoder with Bayesian Optimization. *Energies* **2021**, *14*, 1596. [[CrossRef](#)]
16. Mi, Y.; Liu, C.; Yang, J.; Zhang, H.; Wu, Q. Low-carbon generation expansion planning considering uncertainty of renewable energy at multi-time scales. *Glob. Energy Interconnect.* **2021**, *4*, 261–272. [[CrossRef](#)]
17. Du, E.S.; Sun, Y.L.; Zhang, N.; Chen, S.S.; He, G.X.; Kang, C.Q. Transmission Expansion Planning Model Facilitating Low-Carbon Power Sources' Development. *Power Syst. Technol.* **2015**, *39*, 2725–2730. [[CrossRef](#)]
18. Li, Z.; Chen, S.; Dong, W.; Liu, P.; Du, E.; Ma, L.; He, J. Low Carbon Transition Pathway of Power Sector Under Carbon Emission Constraints. *Proc. CSEE* **2021**, *41*, 3987–4001. [[CrossRef](#)]
19. Writing Group of the General Report. General report of “the transformation strategy and pathway of low carbon development in China”. *China Popul. Resour. Environ.* **2020**, *30*, 1–25. [[CrossRef](#)]
20. Liu, G.; Li, M.; Zhou, B.; Chen, Y.; Liao, S. General indicator for techno-economic assessment of renewable energy resources. *Energy Convers. Manag.* **2018**, *156*, 416–426. [[CrossRef](#)]
21. Abe, J.O.; Popoola, A.P.I.; Ajenifuja, E.; Popoola, O.M. Hydrogen energy, economy and storage: Review and recommendation. *Int. J. Hydrog. Energy* **2019**, *44*, 15072–15086. [[CrossRef](#)]
22. International Renewable Energy Agency. Green Hydrogen: A Guide to Policy Making. Available online: <https://irena.org/publications/2020/Nov/Green-hydrogen> (accessed on 5 November 2022).
23. Noussan, M.; Raimondi, P.P.; Scita, R.; Hafner, M. The Role of Green and Blue Hydrogen in the Energy Transition—A Technological and Geopolitical Perspective. *Sustainability* **2021**, *13*, 298. [[CrossRef](#)]
24. China Hydrogen Alliance. White Paper on China's Hydrogen Energy and Fuel Cell Industry. 2019. Available online: <http://h2cn.org.cn/publicati/215.html> (accessed on 4 November 2022).
25. National Bureau of Statistics of China. 2021 China Statistical Yearbook. Available online: <http://www.stats.gov.cn/tjsj/ndsj/2021/indexch.htm> (accessed on 6 October 2022).
26. Liu, W.J.; Sun, L.; Li, Z.L. Trends and future challenges in hydrogen production and storage research. *Environ. Sci. Pollut. Res.* **2020**, *27*, 31092–31104. [[CrossRef](#)] [[PubMed](#)]
27. Kurtz, J.; Bradley, T.; Winkler, E.; Gearhart, C. Predicting demand for hydrogen station fueling. *Int. J. Hydrog. Energy* **2022**, *45*, 32298–32310. [[CrossRef](#)]
28. Huang, J.; Li, W.; Wu, X. Forecasting the Hydrogen Demand in China: A System Dynamics Approach. *Mathematics* **2022**, *10*, 205. [[CrossRef](#)]
29. Fan, G.F.; Peng, L.L.; Hong, W.C.; Sun, F. Electric load forecasting by the SVR model with differential empirical mode decomposition and auto regression. *Neurocomputing* **2016**, *173*, 958–970. [[CrossRef](#)]
30. Tahmasbi, R.; Hashemi, S.M. Modeling and Forecasting the Urban Volume Using Stochastic Differential Equations. *IEEE Trans. Intell. Transp. Syst.* **2014**, *15*, 250–259. [[CrossRef](#)]